Time-resolved microwave conductivity (TRMC) a useful characterization tool for charge carrier transfer in photocatalysis: a short review

C. Colbeau-Justin
Laboratoire de Chimie Physique, CNRS UMR 8000, Univ. Paris-Sud, 91405 Orsay, France

M. A. Valenzuela
Lab. Catálisis y Materiales, ESIQIE-Instituto Politécnico Nacional,
Zacatenco, 07738, México D.F., México.
e-mail: mavalenz@ipn.mx

Received 4 October 2012; accepted 14 January 2013

We provide a brief introduction about photocatalysis and the reaction mechanism for charge-carrier dynamics focusing in the situation and application of Time Resolved Microwave Conductivity (TRMC) as a useful characterization technique of irradiated semiconductors.

Keywords: Semiconductors; microwave conductivity; photocatalysis.

En el presente trabajo de revisión se describen brevemente los fundamentos de fotocatálisis y los mecanismos de reacción en la dinámica de los portadores de carga enfocándose en el estado y aplicaciones de la conductividad de microondas resuelta en el tiempo (TRMC) como una técnica útil de caracterización de semiconductores irradiados.

Descriptores: Semiconductores; conductividad de microondas; fotocatálisis.

PACS: 81.05.Hd ; 72.20.Jv ; 82.50.Hp

1. Introduction

A new approach to design and control chemical processes at the molecular level has opened new opportunities in the development of new nanocatalysts [1-3], fuel and solar cells [4-6], nanocomposites with special optical, electrical, magnetic and mechanical properties [7-9] and nanoporous materials [10-12], among others. This development has given rise to a new interaction between engineering and molecular sciences trying to understand the relationship between molecular structure and properties [13,14]. The use of novel synthesis methods (*e.g.* physico-chemical methods with the bottom-up approach) as well as the application of conventional and sophisticated characterization techniques for the bulk and the surface of solids has been very useful in order to get new nanomaterials with specific applications [15-17].

As it is well known, chemical process design is based in the concept of unit operations, which have been well described by the fundamentals of transport phenomena [14,18]. Consequently, there are three basic transfer process (*i.e.* momentum, heat and mass transfer) that can be used to explain all unit operations required by the conventional chemical industry [18]. However, as mentioned above, for the new and flourishing processes and products industry involving nanostructure compounds, another fundamental transfer process has completed the crossword which is called *charge-carrier transfer* [19]. Obviously, this concept has been largely used in the fields of electrochemistry, electrostatics and electronics. Nevertheless, thinking in the solution of many problems for new advanced technologies at the molecular level, it is strongly necessary to consider the charge-carrier transfer processes [20].

In particular, catalytic and photocatalytic systems include a complex reaction mechanism involving physical (*e.g.* mass transfer, adsorption, etc;), chemical (*e.g.* surface reaction, poisoning, etc.) but also charge-carrier generation and transport, with or without light irradiation, which must be understood as a whole process with the possibility to determine the controlling step [21]. The starting points to understand the fundamentals of charge-carrier transfer are the band models and transport processes which from a theoretical point of view have been already well established and are out of the scope of this review article [22]. However, it is worth noting

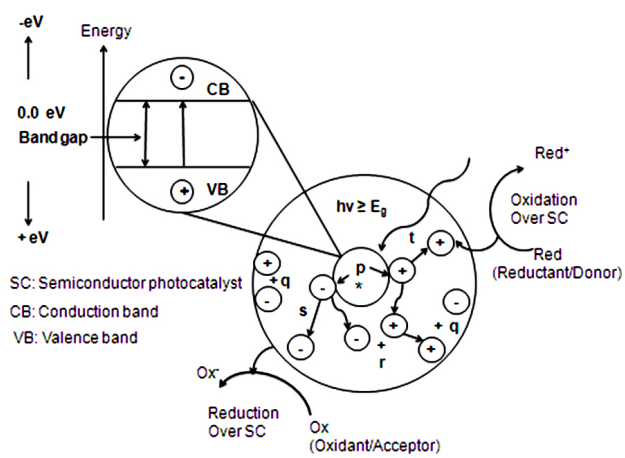

FIGURE 1. Schematic representation of photophysical and photochemical processes over a photon activated semiconductor particle. (p) photogeneration of charge-carriers; (q) surface recombination; (r) recombination in the bulk; (s) diffusion of acceptor and reduction on the surface of the SC; (t) oxidation of donor on the surface of the SC. Adapted with permission from Ref. 24. Copyright 2008 Elsevier.

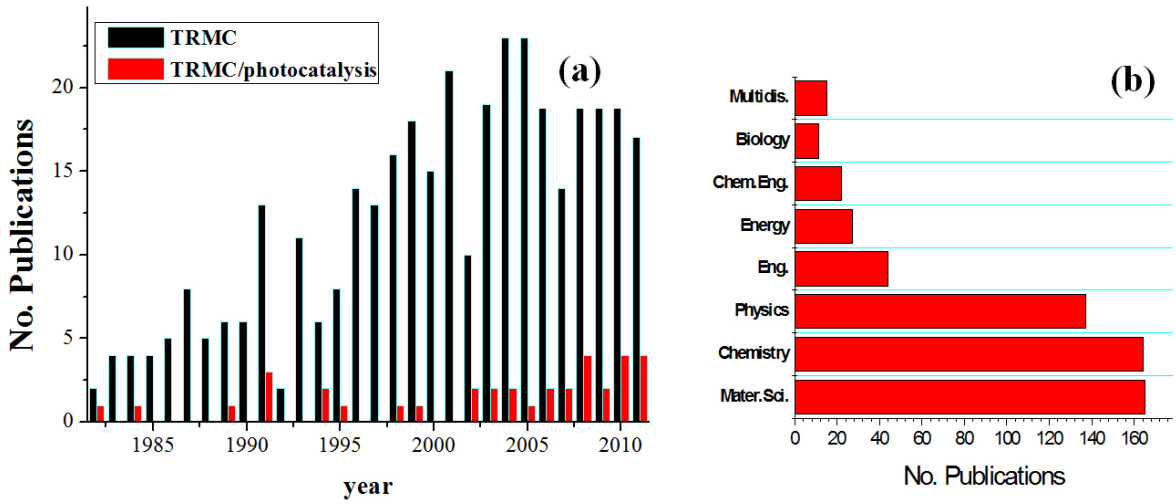

FIGURE 2. Statistics of TRMC data: (a) comparison between papers published in TRMC with those in TRMC/photocatalysis; (b) main disciplines of study of TRMC. Source: Scopus 2011.

that in the electric conduction in solids or charge-carrier transfer, the number of carriers is linked to the generation processes, while the mobility is related to the transport processes. In a photocatalytic reaction, charge-carriers are generated upon light irradiation of a semiconductor, then, can get trapped or recombined or they can take part in several redox reactions, as shown in Fig. 1 [23,24]. These are ultra fast processes occurring on the femto, pico and nano time scales, which are currently studied by time-resolved techniques such as absorption spectroscopy, diffuse reflectance, electron spin resonance, microwave conductivity, among others [25-27].

According to the IUPAC definition, Time Resolved Microwave Conductivity (TRMC) is a technique allowing the quantitative and qualitative detection of radiation-induced charge separation by time-resolved measurement of the changes in microwave absorption resulting from the production and decay of charged and dipolar molecular entities [27]. This is a contactless and noninvasive in situ characterization technique for semiconductors and semiconductors devices that offers the possibility to obtain information on charge-carrier transfer [28-48]. TRMC has been used since the 70's mainly in the characterization of semiconductors with applications in optoelectronics. Charge-carrier recombination dynamics, effective mobility of the carriers formed, carrier lifetimes and trapping, among other information is obtained for the application of this technique [28-48]. In spite of the high amount of published works in fundamental or applied photocatalysis aspects, around 1500 articles per year, a few amounts of works devoted to the characterization of charge-carrier kinetics in semiconductors useful in photocatalysis have been reported, as shown in Fig. 2a. Note in Fig. 2b that most papers have been oriented to the fields of material science, chemistry and physics.

The present work is divided in two parts; firstly, an overview of photocatalysis emphasizing the importance of charge carrier transfer in the reaction mechanism is presented. Thereafter, the fundamentals and equipment of TRMC are described and finally a representative study cases using TRMC linked with semiconductors used in photocatalysis are discussed.

2. Photocatalysis: a brief overview

Semiconductor photocatalysis has been studied extensively since the decade of 70's focusing in the degradation of a great number of pollutants [49,50], water splitting/CO_2 reduction [51,52], and organic syntheses [53,54]. However, a wide range of opportunity for topics in research and development are now being studied mainly with the use of titanium dioxide in all its modalities [50]. For example, a detailed list of areas of application of photocatalysis and its specific topics which are now in research and development steps have recently reported [55]. Note that the photocatalytic degradation of pollutants and the solar energy conversion are both of the major relevance, however, the development of new photocatalytic materials and coatings are impacting as a new flourishing construction industry [55].

Although TiO_2 has been the most used semiconductor due to its inherent photoactivity, photochemical stability, nontoxicity and cost-effective material, it has a serious disadvantage in comparison with other semiconductors that are activated with visible light. A heterogeneous photocatalytic reaction involves the combination of photochemistry and catalysis, meaning that both light and semiconductor material are inevitable to enhance the rate of kinetically slow reactions. For instance, semiconductors used for the photocatalytic degradation of organic molecules are usually metal oxides or metal sulfides that carry out a complete mineralization process:

$$\text{Organic Pollutant} + O_2 \xrightarrow[\text{semiconductor}]{h\nu \geq E_g} \text{mineralized products} \quad (1)$$

This process takes into account the oxidation and reduction potentials as well as the energy of the band gap of the

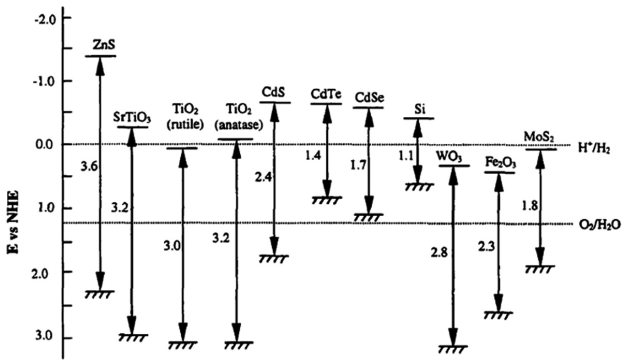

FIGURE 3. Valence and conduction band positions of semiconductors at pH=0. Adapted with permission from Ref. 58. Copyright 2004 American Chemical Society.

semiconductor. The photogenerated valence band holes (h^+_{vb}) are useful to create hydroxyl radicals ($OH^\bullet$) and conduction band electrons (e^-_{cb}) to reduce molecular oxygen to superoxide. The energy of the band gap (E_g) is the energy of light needed to excite an electron to the conduction band and is usually measured in the order of few electron-volts. Figure 4 depicts the valence and conduction band position of some selected semiconductors as well as the relevant redox couples. Note that the position of valence and conduction bands of a semiconductor determines the reaction pathway. For instance, the photo-oxidation and photoreduction of water is possible thermodynamically with CdS (E_g= 2.4 eV), however, if we use Fe_2O_3 with an E_g=2.3 eV, it is only possible to carry out the photo-oxidation reaction. It is worth noting that oxidation and reduction must occur simultaneously due to different couples that can be present and should maintain a photocatalytic cycle. Organic compounds and water are two potential reductants, while oxygen and metal ion are two potential oxidants in photocatalytic process [56]. Some illustrative examples of redox reactions taking place during a true photocatalytic reaction can be found in Ref. 57.

Considering a photocatalytic reaction taking place in aqueous solution, three processes are involved in the system: mass transfer, adsorption/interfacial reactions and ultrafast processes inside the illuminated semiconductor, Fig 4. Indeed, a unified quantitative model for a specific photocatalytic reaction must include all competitive processes that occur from femto- to milliseconds. Focusing in the process oc-

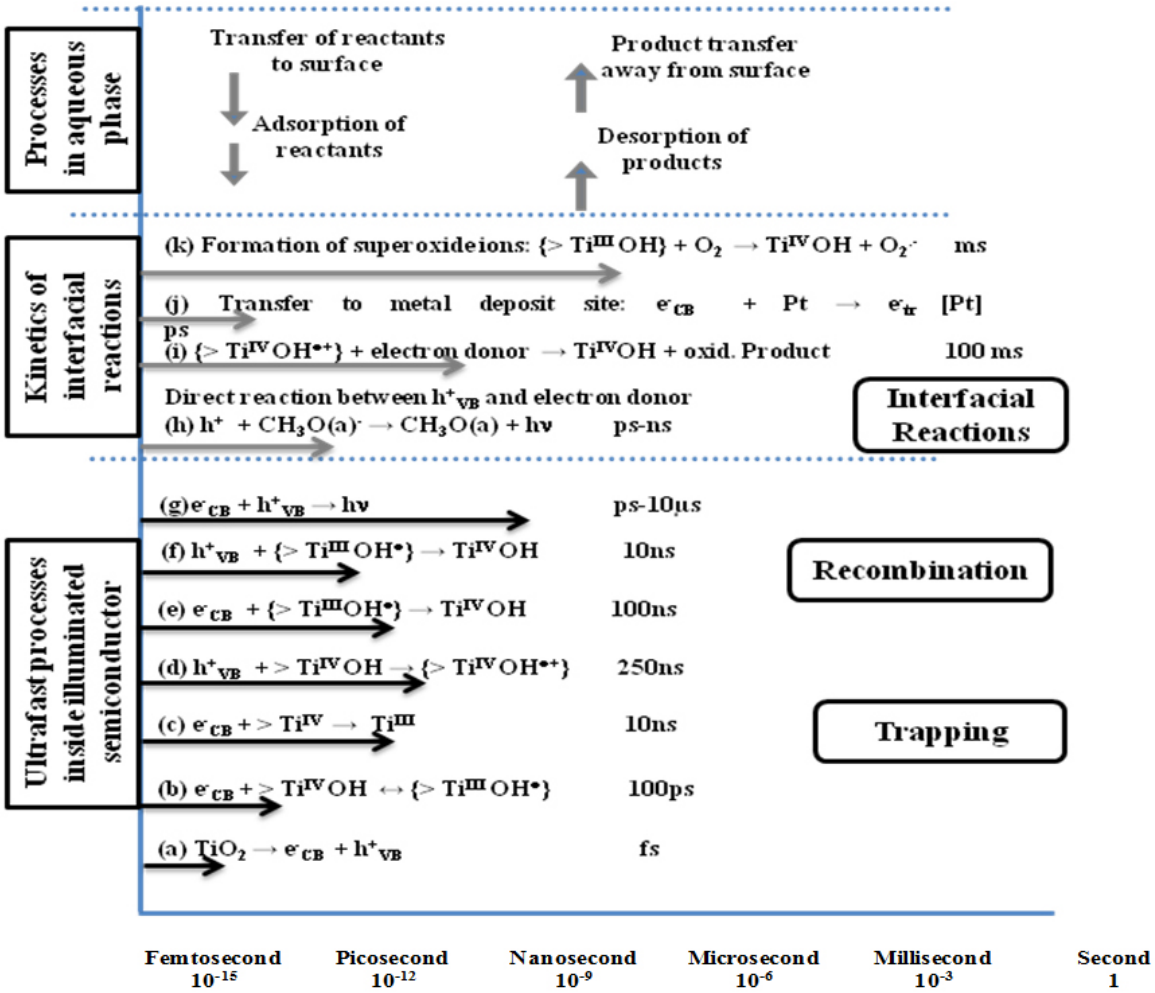

FIGURE 4. Elementary reactions in TiO_2 photocatalysis with corresponding timescales. Adapted with permission from Ref. 23. Copyright 2010 Elsevier.

curring inside the particle (*i.e.* charge-carriers generation, trapping and recombination steps), these reactions take place in the range of femto- to microseconds giving rise to a valuable trapping electrons and holes for the interfacial reactions and of course for the undesirable recombination reaction. This part of the whole process is very useful for the interpretation and understanding of mechanisms in photocatalysis. On the other hand, to build a comprehensive kinetic model (usually the classical Langmuir-Hinshelwood) a deep knowledge of the charge-carriers generation and transport would help to clarify the relationship between the photodegradation rate and the illumination intensity [60]. Several techniques have been used to study the ultrafast processes in illuminated semiconductors and a summary of the most important results is reported in Ref. 23.

Although many efforts have been devoted to study the charge transfer mechanisms in traditional photocatalysts (*e.g.* TiO_2 anatase or rutile phases), it is still difficult to discuss a more sophisticated photocatalytic systems made of thin films of nanotubes or nanowires that exhibit peculiar optical and electronic properties [22]. Therefore, the employment of TRMC method together with other macroscopic techniques and the corresponding kinetic studies using advanced photocatalytic materials irradiated with visible light, offer the possibility for developing promising pollution remediation technologies.

3. Time-Resolved Microwave Conductivity (TRMC)

3.1. Fundamentals

The TRMC [59-61] method is based on the measurement of the change of the microwave power reflected by a sample induced by laser pulsed illumination of this sample. The relative change, (ΔP(t)/P) of the reflected microwave power is caused by a variation $\Delta\sigma$(t) of the sample conductivity induced by the laser. For small perturbations of conductivity, a proportionality between ΔP(t)/P and $\Delta\sigma$(t) has been established:

$$\frac{\Delta P(t)}{P} = A\Delta\sigma(t) = Ae\sum_i \Delta n_i(t)\mu_i \qquad (2)$$

$\Delta n_i(t)$ is the number of excess charge-carriers i at time t, μ_i is the mobility of charge-carrier i. The sensitivity factor A is independent of time, but dependent on the microwave frequency and on the conductivity of sample.

For the present work, the Eq. (2) can be reduced to mobile electrons in the conduction band and holes in the valence band. Trapped species can be neglected because of their small mobility.

$$\frac{\Delta P(t)}{P} = A\Delta\sigma(t) = Ae\left(\Delta n(t)\mu_n + \Delta p(t)\mu_h\right) \qquad (3)$$

$\Delta n(t)$ is the number of excess electrons, μ_n is the mobility of electrons, $\Delta p(t)$ and μ_h are the corresponding properties of holes. The TRMC signal ($\Delta P(t)/P$ or $I(t)$) obtained by this technique is called (microwave) photoconductivity, it allows to follow directly, on the 10^{-9} - 10^{-3} s time scale, the decay of the number of electrons and of the holes after the laser pulse by recombination or trapping of the charge-carriers.

3.2. Equipment

The principle of the measurements is to place the powder sample inside a wave-guide, to proceed to its illumination by a UV pulsed laser, and then to follow the temporal evolution of microwave power reflected by the sample. The incident microwaves are generated by a Gunn diode in the Ka band (28-38 GHz). The experiments are frequently carried out at 31.4 GHz. The reflected microwaves are detected by a Schottky diode. The signal is amplified and displayed on a digitizer [33]

Pulsed light source is a Nd:YAG laser giving an IR radiation at λ = 1064 nm with a 10 Hz frequency. Full width at half-maximum of one pulse is 10 ns. UV light is obtained by tripling (355 nm) or quadrupling (266 nm) the IR radiation. The maximum light energy density received by the sample is 1.3 mJ/cm^2 for both wavelengths.

3.3. Study cases

In order to get a better understanding of the correlation between structural, textural and electronic properties of TiO_2 powders and their photocatalytic activities, the photocatalysis mechanism must be considered separately in two linked parts (photo and catalysis). The first part (photo part) concerns phenomena linked to light-materials interaction which includes photons absorption, charge-carrier creation and dynamics, and also surface trapping. The second part (catalysis part), concerns phenomena linked to surface radicals formation and surface reactivity *i.e.* the interaction between H_2O, O_2, organic pollutant and the oxide surface.

For the photo part, the most effective structural parameter on photocatalysis is the crystalline quality [36]. Actually, the oxidant radicals, which are the active species in photocatalysis are formed when the charge-carriers created by absorbed UV-photons are trapped in the surface. Thus, recombination and bulk trapping phenomena that decrease charge-carrier lifetimes and prevent their arrival to the surface, penalize the formation of the oxidant radical. Yet, recombination and bulk trapping are promoted by defects, doping elements, and impurities or amorphous domains. Consequently, to enhance the charge-carrier lifetimes, the crystalline quality should be as high as possible. Thus, for titania, the TRMC measurements can be considered as indicator of the level of crystalline quality. High values of $I_{\max}$ and slow decay indicate an important amount of charge-carriers created with long lifetimes, and reveal a high crystalline quality.

For the catalysis part, the specific surface area is the most effective structural parameter. Indeed, photocatalysis is an interfacial reaction. Thus, higher specific surface area induces

TABLE I. TRMC studies on TiO_2 and other photocatalysts.

Photocatalyst	Type of study	Comments	Year [Ref.]
$MoSe_2$, MoS_2 and platinized or halogenated samples	Effect of Pt and halogens on the dynamics of excess charge carriers	Pt/ $MoSe_2$ and halogens/ MoS_2 dramatically shorten the lifetimes of excess charge carriers	1990 [28]
Al_2O_3, MgO, TiO_2 powders	Mobility evaluation and charge-carrier dynamics obtained by electronic irradiation.	Influence of Pt covering, isopropanol and Cr^{3+} doping	1991 [29]
TiO_2 (Degussa P25)	Full understanding of the bulk and surface electronic processes taking place in suspensions of TiO_2	Charge recombination is retarded in presence of isopropanol due to surface hole scavenging	1991 [30]
TiO_2 (Degussa P25), Q-TiO_2, Fe^{3+}-doped Q-TiO_2	Charge carrier recombination dynamics and photo-oxidation of chloroform	TRMC conductivity signals were assigned to electrons remaining in the semiconductor lattice after hole transfer. The electron-transfer rates were consistent with the photoreactivity results	1994 [31]
TiO_2 (Degussa P25), Q-TiO_2	Effect of adsorbates (inorganic, organic) and light intensity on charge-carrier dynamics	Charge carrier dynamics results showed a different photoelectro-chemical mechanisms of TiO_2 and Q-TiO_2	1994 [32]
Nanocrystalline porous TiO_2 films	Influence of chemical treatments on the photoinduced charge carrier kinetics	An increase in the photogenerated charge carrier concentration as well as a decrease in the recombination process was detected by the chemical treatments with Ti isopropoxide or $TiCl_4$	2003 [33]
TiO_2 (rutile doped with Cr and Nb and anatase)	Effect of doping and thermal treatments on charge-carrier lifetimes	Doping favored charge carrier recombination. Thermal treatments of anatase at high temperatures increased the lifetimes	2003 [34]
TiO_2 prepared by sol-gel (xero and aero gels)	Effect of the preparation method on opto-electronic and photocatalytic properties	TiO_2 aerogels treated at high temperatures showed the highest lifetimes and photocatalytic conversion of phenol	2004 [35]
Nanocrystalline TiO_2 prepared by hydrothermal method	Effect of the preparation method on opto-electronic and photocatalytic properties	The highest lifetime and photocatalytic conversion of phenol was found with sample containing 15% rutile +85%anatase	2004 [36]
TiO_2 and dye-sensitized nanocrystalline TiO_2	Determination of trap density, decay kinetics and charge separation efficiency under UV and Vis light	The mobility of electrons within the TiO_2 matrix are independent of dye addition	2004 [37]

TABLE I. (Cont.)

Photocatalyst	Type of study	Observations	Year [Ref.]
TiO_2 , porphyrin-TiO_2, Cu-porphyrin- TiO_2	Determination of the number and lifetimes of the photoinduced excess charge carriers	The presence of macrocycles increases the number and lifetime of the charge carriers which correlates with the photocatalytic activity	2005 [38]
Commercial TiO_2 (Degussa P25, Sachtleben UV100, Millennium PC50) and platinized forms	Study of charge-carrier dynamics related with photocatalytic activity	With Pt samples; at short times fewer charge carriers are formed which recombine faster; at long times, platinization had different effects depending the type of TiO_2	2006 [39]
Dye-sensitized nanocrystalline TiO_2	Effect of the particle size on the electron injection efficiency	Dye adsorbed on 20 nm TiO_2 had 100% injection efficiency, attributed to an increase in electron mobility (by occupation of traps)	2007 [40]
TiO_2 P25 powder and films	Effect of surface treatments on opto-electronic properties	Surface treatment by adsorption of oxalic acid increases the decay. TiO_2 powders and films presented the same behaviour	2007 [41]
TiO_2 (P25 and sol-gel) modified with Pt ions and Pt clusters	Effect of type of TiO_2 and Pt precursor on optoelectronic and photocatalytic properties	Under UV irradiation platinum acts as a charge scavenger hindering charge recombination.	2008 [42]
CdS-coated mesoporous $TiO_2$and ZrO_2	Photoinduced charge injection from CdS to TiO_2 and ZrO_2	There was no injection of electrons from CdS to ZrO_2. The quantum yield for electron injection in TiO_2 was close to unity	2008 [43]
TiO_2 Hombikat UV100, Au/TiO_2	Effect of Au deposition on the opto-electronic properties of TiO_2	High electron affinity of Au lowers the lifetime of mobile electrons	2009 [44]
nanocrystalline TiO_2 films sensitized with black dyes	Quantitative study of solvent effect on electron injection efficiency	Acetonitrile had the highest efficiency. Results were explained in terms of interactions between the black dye and the –CN groups of the solvent	2009 [45]
TiO_2 Hombikat UV100 calcined from 200 to 800°C	Determination of opto-electronic properties	Samples with particle sizes up to an average of 15 nm contain a large concentration of trapping sites	2010 [46]
TiO_2 Hombikat UV100, Au/TiO_2	Determination of opto-electronic properties at 300 and 530 nm	Gold does not induce visible light activity of anatase	2011 [47]
TiO_2 Millennium PC series modified with Pd nanoparticles	Study of charge-carrier dynamics related with photocatalytic activity	Pd does not induce visible light activity, but increases UV light activity	2012 [48]

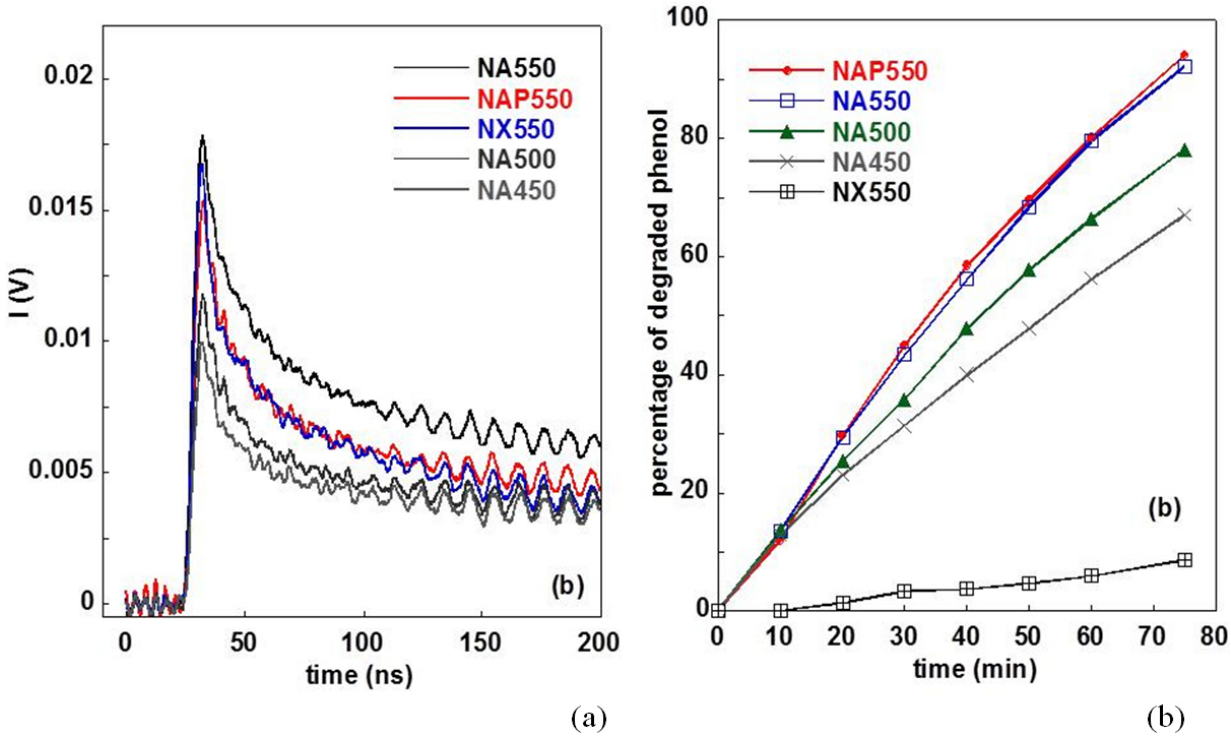

FIGURE 5. (a) TRMC signals on TiO_2 powders - (b) Evolution of percentage of photodegradated phenol in time. Adapted with permission from Ref. 35. Copyright 2004 Elsevier.

higher number of accessible active sites and consequently better reactivity. Some works have used the TRMC method to understand the relation between synthesis conditions, structural and microstructural parameters, and photoactivity. Table I shows several studies reported from 1990 to 2012 where charge-carrier dynamics related with photocatalytic activity were followed by TRMC. Indeed, most studies are devoted to titania (mainly, Evonik, ex-Degussa P25) but also advanced TiO_2 nanostructures modified by small amount of metal and composite semiconductors are included.

TRMC preliminary studies were focused to understand the charge transfer kinetics in terms of charge-carrier generation, charge-carrier trapping, charge carrier recombination, and electron and hole transfer. Moreover, recent studies are aimed to know the relationship between the transfer and separation of the charge carriers on the enhancement of the photocatalytic efficiency. The effect of preparation method of the semiconductor, the addition of noble metals and the study of plasmonic structures as well as graphene semiconductor interaction are important ways to enhance the charge separation and to suppress the recombination.

The next section will be devoted to discuss our work in the synthesis of TiO_2, the characterization by TRMC and its correlation with photocatalytic activity.

3.4. Supercritical drying [35]

Various TiO_2 powders have been synthesized by sol-gel method followed by drying in supercritical CO_2 (areogels). The properties of these powders were compared to those of other powders elaborated by classical sol-gel method (xerogels). Comparatively to the other synthesis parameters (sol-gel parameters, thermal treatment...), the drying procedure seems to be the most influential on the final properties of TiO_2 powders. Both, structural and photocatalytic properties are dramatically modified by the drying method.

Thus, the crystallite diameter of xerogels is perceptibly higher than that of aerogels, and the corresponding specific

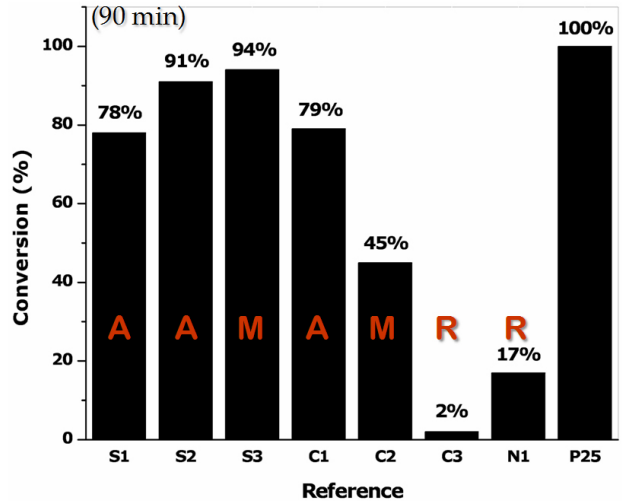

FIGURE 6. Degree of degraded phenol after 90 min illumination. Adapted with permission from Ref. 36. Copyright 2004 Elsevier.

TABLE II. Phase composition and surface area of titania synthesized by hydrothermal method. Adapted from Ref. 36.

Reference	Precursor, T, t	Phase composition of synthesized samples	BET m^2/g ($\pm$5%)
S1	$TiOSO_4$250°C, 6 h	Anatase 100%	79
S2	$TiOSO_4$,250°C, 10 min	Anatase 100%	43
S3	$TiOSO_4$,250°C, 6 h	Anatase-85% Rutile-15%	78
C1	$H_2TiO(C_2O_4)_2$, 250°C, 6 h	Anatase 100%	25
C2	$H_2TiO(C_2O_4)_2$, 250°C, 10 min	Anatase-95% Rutile-5%	43
C3	$H_2TiO(C_2O_4)_2$, 150°C, 6 h	Rutile 100%	79
N1	$TiO(NO_3)_2$, 250°C, 6 h	Rutile-95% Anatase-5%	22

surface areas are very low. The catalysis aspect is therefore, clearly promoted by supercritical drying. Nevertheless, the TRMC results show that the electronic properties depend on the nature of the gel. The photo aspect may be promoted or slightly damaged by supercritical drying.

In the case of a nitric acid based gel (N-series), the surface areas of the aerogel (NA550) and xerogel (NX550) are, respectively, 63 m^2/g and 3 m^2/g. Figure 5a shows that NA550 presents a higher and slower TRMC signal compared to NX550 which evidences more charge-carriers with longer lifetimes in the aerogel. The supercritical drying clearly promotes both, photo and catalysis parts, explaining the important difference in the phenol photodegradation observed on Fig. 5b As can be seen, 8.7 and 92.2%, of degradation after 75 min of illumination was obtained for NX550 and NA550. In the case of a hydrochloric acid based gel (C-series), the TRMC shows a weak decrease of the electronic properties which is not enough to go against the improvement of photocatalytic properties by supercritical drying.

3.5. Hydrothermal synthesis [36]

Nanocrystalline titania has been prepared by hydrothermal treatment of aqueous $TiOSO_4$, $H_2TiO(C_2O_4)_2$, and $TiO(NO_3)_2$ solutions. The photoactivity of the obtained powders has been evaluated on phenol photodegradation (Fig. 6) and interpreted in terms of structural (Table II) and electronic properties using TRMC (Fig. 7).

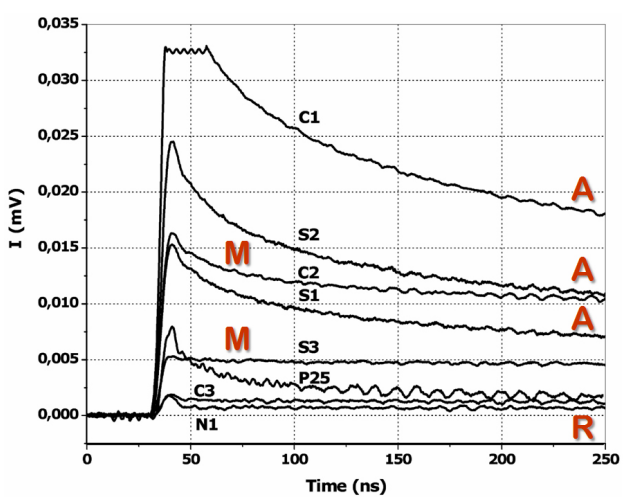

FIGURE 7. TRMC signals on TiO_2 powders. Adapted with permission from Ref. 36. Copyright 2004 Elsevier.

S1, S2 and C1 are pure anatase samples. Concerning the photo part, the TRMC evidences three parallel decays with different intensities. C1 shows the best crystalline quality, then S2 and follows S1. Concerning the catalysis part, the opposite order is observed, S1 shows the best surface area, then S2 and follows C1. The photocatalytic activity is the result of these two combined parameters. S2 presents the best "average" crystalline quality and specific surface, its activity is higher than those of S1 and C1.

N1 and C3 are mostly rutile samples. In this case, the specific surface does not play any role. The photo part is the dominant effect. The rutile crystal structure implies a lower mobility of charge-carriers than in anatase structure. This explains the TRMC measurements showing that the charge-carriers recombine during the pulse and are not available for photocatalysis. The low value of activity observed with N1 sample is due to the small amount of anatase phase.

C2 and S3 samples mostly contain anatase but have an admixture of rutile (95/5 and 85/15 % anatase/rutile respectively). As explained above, rutile itself is a low-active phase. However, commercial TiO_2 P25 (Evonik), considered as one of the best photocatalyst, is also a mixture (75% anatase - 25% rutile) and good interparticle contacts are formed between anatase and rutile particles in water. The junction created by the two semiconductors helps the charge-carrier separation. It means that the carriers created in the rutile part do not rise up photoactivity like in the pure phase. The rutile phase of P25 plays only the role of charge separator and provides sites for oxidation. As described above, this separation of charge-carriers could take place for C2 and mainly for S3 samples.

The synthesized C2 powder morphology is constituted of not hard-grained aggregates containing separated rutile and anatase nanoparticles. Probably, this kind of aggregation does not allow creating the charge-carriers separation in C2 like in the case of P25. In addition, C2 contain only $\sim$5% of rutile. This fact is confirmed by TRMC experiment. The number of charge-carriers created is not very large compared

to pure anatase samples; the effect of the rutile phase is measured on the decay but may not be really influent because recombination phenomena during the pulse are still observed. Furthermore, its specific surface is average (43 m^2/g). The activity of C2 is lower than that of C1, S2 or S1.

In the case of S3 (15% rutile),this sample consists of hard-grained aggregates of separated rutile and anatase nanoparticles. It supposes that in S3 sample good contacts are formed between anatase and rutile particles similarly to P25. This is confirmed by TRMC experiment. The number of charge-carriers created is not very high but the effect of rutile phase on the decay is quite essential. The created charge carriers have a long lifetime. Almost no recombination during the pulse is observed. Taking into account the high specific surface area of this sample (78 m^2/g), it is believable that S3 is the best photocatalyst among the samples obtained by hydrothermal method.

4. Conclusions

Semiconductor photocatalysis has been exhaustively studied in the last three decades for many applications. Currently, there are already successful commercial applications in the field of environment and energy. However, hot topics such as water splitting and CO_2 photoconversion (artificial photosynthesis) remain elusive despite numerous research works. In general, efficiency improvements for the photocatalytic reactions are highly expected by the use of new advanced nanostructured materials able to work with visible light.

This review has highlighted the importance of charge-carrier transfer process in a photocatalytic reaction and the relevance to the global efficiency. Specially, charge-carrier generation, trapping and recombination, ultrafast processes that occur at very short times (femto-nano seconds) after irradiation of semiconductors, have a marked influence on the photocatalytic efficiency. TRMC studies reported here have focused on studying the charge transfer kinetics on photocatalytic reactions using TiO_2 and other semiconductors as a tool to understand how it could be increased efficiency.

Acknowledgments

The present research was supported by CONACYT – Project No. 153356 and SIP-IPN No. 20123458. MAV gratefully thanks for the warm hospitality extended to him at the Laboratoire de Chimie Physique of the Université Paris-Sud, France.

1. A. Z. Moshfegh, *J. Phys. D: Appl. Phys*. **42** (2009) 233001.
2. B. Roldan Cuenya, *Thin Solid Films* **518** (2010) 3127.
3. S. B. Kalidindi and B. R. Jagirdar, *ChemSusChem*. **5** (2012) 65.
4. F. Jaouen *et al*., *Ener. Environ. Sci*. **4** (2011) 114.
5. J. Yum, P. Chen, M. Grätzel, and M.K.Nazeeruddin, *Chem. Sus. Chem*. **1** (2008) 699.
6. B. D. Alexander, P. J. Kulesza, I. Rutkowska, R. Solarska, and J. Augustynski, *J. Mater. Chem.* **18** (2008) 2298.
7. R. Pfaendner, *Polymer Degrad.Stab*. **95** (2010) 369.
8. C. Sanchez, B. Leveau, F. Chaput, and J. P. Boilot, *Adv.Mater*. **15** (2003) 1969.
9. M. Orilall, M. Christopher, and W. Ulrich, *Chem.Soc.Rev*. **40** (2011) 520.
10. G. A. Tompsett, W. C. Conner, and K. S. Yngvesson, *Chem. Phys. Chem* **7** (2006) 296.
11. J. Jianwen, B. Ravichandar and H. Zhongqiao, *Chem. Soc. Rev* **40** (2011) 3599.
12. S. Polarz and B. Smarsly, *J.Nanoscience Nanotech*. **2** (2002) 581.
13. H. M. Chawla, *Introduction to Molecular Engineering* (CRC Press; Boca Raton, FL, 2007).
14. E. L. Cussler and G. D. Moggridge, *Chemical Product Design* (Cambridge University Press: Cambridge, U.K. 2001).
15. X. Lu, M. Rycenga, S. E. Skrabalak, B. Wiley, and Y. Xia, *Annu. Rev. Phys. Chem*. **60** (2009) 167.
16. K. Maeda *et al*., *Chem. Eur. J*. **16** (2010) 7750.
17. W. Abidi and H. Remita, *Recent Patents on Engineering* **4** (2010) 170.
18. R. B. Byrd, W. Stewart, and W. E. Lightfoot, *Transport Phenomena* (Wiley: New York 2002).
19. V. Balzani, *Electron Transfer in Chemistry*, (ed.) Wiley-VCH: Weinheim, (2001).
20. D. M. Adams *et al*., *J. Phys. Chem. B*, **107** (2003) 6668.
21. B. Ohtani, *J. Photochem.Photobiol.C: Photochem. Rev*. **11** (2010) 157.
22. J. Tyczkowski, *Ind.Eng.Chem.Res*. **49** (2010) 9565 and references therein.
23. D. Friedmann, C. Mendive, and D. Bahnemann, *Appl.Catal. B :Env*. **99** (2010) 398.
24. U. I. Gaya, and A. H. Abdullah, *J.Photochem.Photobiol. C:Photochem.Rev*. **9** (2008) 1.
25. G. Rothenberger, J. Moser, M. Graetzel, N. Serpone, and D. K. Sharma, *J.Am.Chem.Soc*. **107** (1985) 8054.
26. D. W. Bahnemann, M. Hilgendorff, and R. Memming, *J.Phys.Chem.B* **101** (1997) 4265.
27. IUPAC *Compendium of Chemical Terminology* **68** (1997) 2280.
28. K. M. Schindler, M. Bikholz, and M. Kunst, *Chem.Phys.Lett*. **173** (1990) 513.
29. J. M. Warman *et al.*, *Int. J. Rad. Appl. Instr. C*. **37** (1991) 433.
30. J.M. Warman, M. P. de Haas, P. Pichat, and N. Serpone, *J.Phys.Chem*. **95** (1991) 8858.

31. S. T. Martin, H. Herrmann, W. Choi, and M. Hoffmann, *J.Chem.Soc.Faraday.Trans*. **90** (1994) 3315.

32. S. T. Martin, H. Herrmann, and M. Hoffmann, *J.Chem.Soc.Faraday.Trans*. **90** (1994) 3323.

33. C. Colbeau-Justin, M. Kunst, and D. Huguenin, *J. Mater. Sci*. **38** (2003) 2429.

34. Y. Lin, X. R. Xiao, W. Y. Li, W.B. Wang, X. P. Li, and J. Y. Cheng, *J.Photochem.Photobiol. A : Chem.* **159** (2003) 41.

35. S. Boujday, F. Wünsch, P. Portes, J. F.Bocket, and C. Colbeau-Justin, *Sol. Ener. Mater.Sol.Cells* **83** (2004) 421.

36. Y. V. Kolenko, B. R. Churagulov, M. Kunst, L. Mazerolles, and C. Colbeau-Justin, *Appl.Catal. B :Env.* **54** (2004) 51.

37. J.E. Kroeze, T.J. Savenije, and J.M. Warman, *J.Am.Chem.Soc*. **126** (2004) 7608.

38. G. Mele *et al*., *J.Phys.Chem. B,* **109** (2005) 12347.

39. C. A. Emilio, M.I. Litter, M. Kunst, M. Bouchard, C. Colbeau-Justin, *Langmuir*, **22** (2006) 3606.

40. R. Katoh, A. Huijser, K. Hara, T. M. Savenije, and L. D. A. Siebbeles, *J.Phys.Chem. C* **111** (2007) 10741.

41. M. Kunst, F. Goubard, C. Colbeau-Justin, and F. Wünsch, *Mater.Sci.Eng.C* **27** (2007) 1061.

42. E. Kowalska, H. Remita, C. Colbeau-Justin, J. Hupka, and J. Belloni, *J.Phys.Chem. B.* **112** (2008) 1124.

43. J. Piris *et al.*, *J.Phys.Chem. C* **112** (2008) 7742.

44. R. Katoh, M. Kasuya, A. Furube, N. Fuke, N. Koide, and L. Han, *Sol. Ener. Mater.Sol.Cells*, **93** (2009) 698.

45. J.T. Carneiro, T.J. Savenije, J.A. Moulijn, and G. Mul, *J.Phys.Chem. C* **114** (2010) 327.

46. R. Katoh, A. Furube, K.I. Yamanaka, and T. Morikawa, *Phys.Chem.Lett.* **1** (2010) 3261.

47. J.T. Carneiro, T.J. Savenije, J.A. Moulijn, and G. Mul, *J.Photochem.Photobiol. A: Chem*. **217** (2011) 326.

48. O. Tahiri Alaoui *et al*., *J. Photochem. Photobiol. A: Chem* **242** (2012) 34

49. D.M. Blake, *Bibliography of Work on the Heterogeneous Photocatalytic Removal of Hazardous Compounds from Water and Air*, Update Number 3 to January 1999, National Renewable Energy Laboratory, USA.

50. O. Carp, C. L. Huisman, and A. Reller, *Prog. Solid State Chem*. **32** (2004) 33.

51. X. Chen, S. Shen, L. Guo, and S. S. Mao, *Chem. Rev*. **110** (2010)6503.

52. A. Mills, and M.A. Valenzuela, *Rev.Mex.Fis*. **50** (2004) 287.

53. M.A. Valenzuela, E. Albiter, O.Rios-Berny, I.Cordova, and S.O.Flores, *J.Adv.Oxid.Tech*. **13** (2010) 321.

54. Y. Shiraishi, and T. Hirai, *J.Photochem.Photobiol.C:Rev*. **9** (2008) 157.

55. W. Choi, *Catal. Surv. Asia* **10** (2006) 16.

56. D. Chen, M. Shivakumar, and A.K. Ray, *Dev. Chem. Mineral Process*. **8** (2000) 505.

57. M. I. Litter, *Appl. Catal. B: Env.* **23** (1999) 89.

58. T.L. Villarreal, R. Gomez, M. Gonzalez, and P. Salvador, *J. Phys. Chem. B* **108** (2004) 20278.

59. M. Kunst and G. Beck, *J. Appl. Phys*. **60** (1986) 3558.

60. M. Kunst and G. Beck, *J. Appl. Phys*. **63** (1988) 1093.

61. J. M. Warman and M. P. De Haas, *in Pulse Radiolysis* (Chapter 6, CRC Press 1991) p. 101.